Vesicular layers in silicon produced by high-dose helium ion implantation

© P.A. Alexandrov, S.G. Shemardov, A.L. Vasiliev, V.N. Beklemishev, A.V. Beklemisheva¶

National Research Center „Kurchatov Institute“,
Moscow, Russia

¶ E-mail: Annabekl@ya.ru

Received February 10, 2026
Revised February 18, 2026.
Accepted March 12, 2026

The development of radiation-induced blistering during high-dose helium ion implantation into a silicon substrate is considered. A method for producing a „buried“porous layer without mechanically damaging the surface silicon is proposed.

Keywords: helium ion implantation, single-crystal silicon wafers, subcritical implantation dose, SOI, buried layers of high porosity.

DOI: 10.61011/SC.2026.01.63727.9086

1. Introduction

The implantation of helium ions into silicon to produce pores (voids) in the bulk of the material has been well studied for the case of irradiation with low doses (generally, up to $5 \cdot 10^{16}\,\mathrm{He^+/cm^2}$). The processes of formation of helium-vacancy complexes and growth of helium microbubbles, the outdiffusion of helium, the formation of pores and mechanisms of their diffusion are understood [1–12]. A quite different situation occurs when implanting large doses ($> 3 \cdot 10^{17}\,\mathrm{He^+/cm^2}$), when the phenomena of amorphization, radiation blistering, presence of critical implantation dose, etc. appear [7,8,13]. Today, there is a need for a more profound study of these processes, since the implantation of helium ions is very beneficial for obtaining silicon-on-insulator structures using the gettering properties of pores during high-temperature internal oxidation of the porous structure and its transformation into a buried dielectric layer [4,10].

2. Problem formulation

During implantation of helium ions, elastic collisions with substrate atoms generate numerous vacancies and interstitial atoms in concentrations several orders of magnitude higher than equilibrium values. These point defects are mobile in silicon even at room temperature and can either recombine with each other or form some vacancy clusters. It is believed that the interaction of helium with divacancies and small vacancy clusters stabilizes them against recombination with silicon interstitials and leads to the formation of helium-vacancy complexes, which then evolve into microbubbles [5,6].

The surface of the samples was examined using a scanning electron-ion microscope Scios (ThermoFisher Scientific, USA).

With implantation doses of $> 1 \cdot 10^{16}\,\mathrm{He^+/cm^2}$ for energies of 40−50 keV, gas bubbles are formed directly during implantation. Increased implantation dose results in larger sizes of gas bubbles and their density increase.

Further transformation of the implantation layer is observed during subsequent annealing. The implanted helium leaves the silicon over a wide range of temperatures, depending on the complexity of the defect that has captured it. At temperatures of 200−300 °C, helium is released from small vacancy complexes and from interstitials, and it can either leave the silicon or be captured by larger defects. As the annealing temperature increases to 800 °C, helium begins to leave the gas bubbles, leaving behind voids (pores). With a further increase in temperature, an enlargement of pores is observed as per migration/coalescence mechanism and (or) Ostwald mechanism [7].

The porosity of the buried synthesized layer (total relative volume of pores per unit volume) is determined by the initial volume of gas bubbles and the amount of helium in vacancy complexes and interstitials. Therefore, increasing the implantation dose is a direct solution to increasing the porosity of the buried layer and, consequently, its resistance.

However, the pressure in gas bubbles leads to the occurrence of stress in silicon, and when the strength parameters of the material are exceeded, mechanical damage to the surface is observed: blistering (swelling of the surface layer) and flakes (peeling of large areas of the surface). Thus, there are limitations on the maximum implantation dose and, as a consequence, on the maximum porosity of the synthesized buried layer.

To solve the problem of implanting large doses of helium ions into silicon, the authors propose a method of subcritical implantations and subsequent annealing. Subcritical is any dose that does not cause mechanical damage to the surface upon subsequent annealing. Annealing is carried out at a temperature of > 800 °C to completely remove the embedded helium from the substrate material. Then the cycle (implantation + annealing) is repeated the required number of times.

3. Equipment and method of the experiment

Single-crystal silicon wafers (100) were irradiated with helium ions using ILU-100 setup (Russia), implantation energy — 50 keV. To prevent mechanical damage to the surface silicon, a method of successive subcritical implantations and anneals was used. Subcritical implantation dose — $1 \cdot 10^{17}\,He^+/cm^2$. Annealing temperature — 1000 °C. The cycle (implantation + annealing) was repeated several times to achieve the required dose.

Sections for the transmission electron microscopy (TEM) studies were prepared using an ion beam in a scanning electron-ion microscope HelisosNanoLab^{tm}600i (USA). Cross-sections were examined using TEM methods on Osiris microscope (USA).

4. Experimental results

Our previous studies have shown that blistering and flecking are observed immediately after implantation of the dose $3 \cdot 10^{17}\,He^+/cm^2$ and after annealing for the dose $2 \cdot 10^{17}\,He^+/cm^2$ [8], while the latest results evidence that the annealing temperature can be extremely low (550 °C).

It should be underscored that the provided results are valid for the implantation and annealing parameters given above. Changes in implantation and annealing conditions can alter the critical implantation dose values and the buried porous layer synthesis process. The last dose at which no mechanical damage to the surface was guaranteed to be observed was $1 \cdot 10^{17}\,He^+/cm^2$. It was this dose that was chosen as the subcritical dose in the method of successive implantations and subsequent annealing.

Calculations using SRIM-2013 software demonstrate that maximal concentration of the implanted helium ions is achieved at a depth of ~ 460 nm, while for the dose $1 \cdot 10^{17}\,He^+/cm^2$ it corresponds to 8.7 at.% (Figure 1).

Scanning electron microscopy was used to evaluate the quality of surface samples obtained by subcritical implantation and subsequent annealing. It showed that the surface of all samples is smooth, no traces of blistering and/or flecking were observed even for a total implantation dose of $3 \cdot 10^{17}\,He^+/cm^2$ (three cycles of implantation of a dose of $1 \cdot 10^{17}\,He^+/cm^2$ and annealing of 1000 °C) (Figure 2).

Cross-sections of samples for total implantation doses $1 \cdot 10^{17}\,He^+/cm^2$ (Figure 3, *a*), $2 \cdot 10^{17}\,He^+/cm^2$ (Figure 3, *b*), $3 \cdot 10^{17}\,He^+/cm^2$ (Figure 3, *c*), obtained by method of subcritical implantation doses and subsequent annealing, have a similar distribution by depth.

The presented figures have a similar distribution of pore depth. Higher implantation doses lead to an enlargement of the pores throughout the crystal and enhanced porosity, especially in the layer which is behind the surface by 360–480 nm, where particularly large pores are concentrated and the average diameter for a dose of $3 \cdot 10^{17}\,He^+/cm^2$ is 90 nm for this region. The lower boundary of this zone coincides with the concentration maximum of the initially implanted helium ions. Thus, different mechanisms of pore formation in the depth of the material are observed.

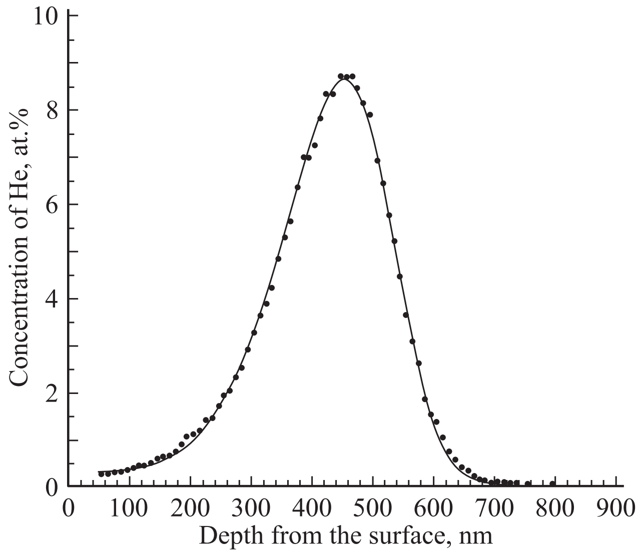

Figure 1. Profiles of the distribution of helium ion concentrations depending on the depth of occurrence inside a silicon sample.

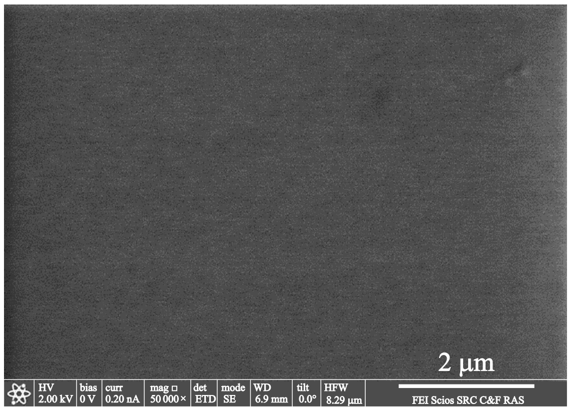

Figure 2. Scanning electron microscopy of the surface of a sample implanted using subcritical dose method and subsequent annealing. Third cycle (dose $3 \cdot 10^{17}\,He^+/cm^2$ and annealing 1000 °C).

In the upper part of the initial concentration profile of helium ions, a moderate growth of pores to a diameter of 10–20 nm is observed, while in the lower part of the profile the pores disappear almost completely, leading to the formation of huge pores in the region of the initial concentration maximum.

In [9] it is shown that recrystallization of the amorphous region obtained as a result of implantation of a large dose ($2.5 \cdot 10^{17}\,He^+/cm^2$) leads to the formation of large gas bubbles (~ 100 nm).

The authors did not conduct any special studies of amorphous zones occurence in the crystal after implantation of $1 \cdot 10^{17} He^+/cm^2$ dose although in this case, near the maximum of distribution, extremely high stresses, close to

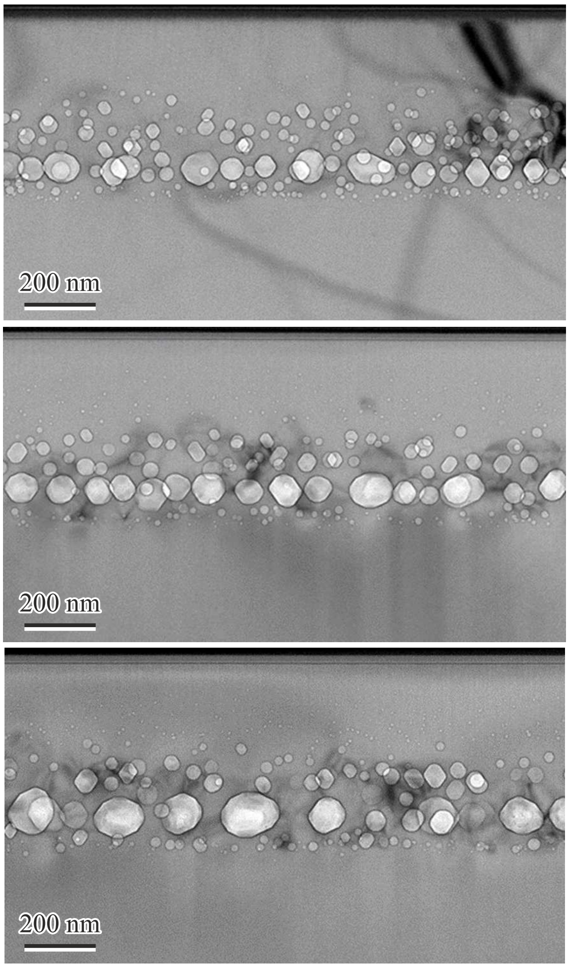

a

b

c

Figure 3. Transmission electron microscopy of the sections of samples implanted by subcritical dose method and subsequent implantations: *a* — first cycle (dose $1 \cdot 10^{17} He^{+}/cm^{2}$ and annealing 1000 °C), *b* — second cycle (dose $2 \cdot 10^{17} He^{+}/cm^{2}$ and annealing 1000 °C), *c* — third cycle (dose $3 \cdot 10^{17} He^{+}/cm^{2}$ and annealing 1000 °C).

the maximum possible, and the possible onset of plastic strain should be expected, which should result in occurrence of a highly defective silicon zone. At low annealing temperatures (up to 500 °C), this dose can expand into the crystal, since defective silicon prevents the diffusion of point defects and helium, interstitial and resulting from the breakdown of small helium-vacancy complexes. If we take into account the larger concentration gradient of the distribution curve's inner branch, then it is possible to spread the highly defective region over its greater part. At temperatures of 550–600 °C, recrystallization processes are activated and the recrystallization front pushes helium and gas bubbles from the depths of the crystal to the top of defective region, leading to the formation of huge gas bubbles. At the same time, in the area adjacent to the surface, the usual processes associated with the out-diffusion of helium and its capture by helium bubbles occur, which we observe for the small dose implantation. The diffusion of helium from gas bubbles and the processes of coalescence of pores (voids) at temperatures 800–1000 °C provide a pattern we observe in Figure 3.

5. Conclusion

The presented method of subcritical implantations and annealings allows the formation of buried layers of high porosity without mechanical destruction of surface silicon.

Funding

This work was supported by the National Research Center „Kurchatov Institute" R & D Center „Development of new implantation methods for producing dielectric intermediate layers in semiconductor substrates for control systems of thermonuclear facilities".

Conflict of interest

The authors declare that they have no conflict of interest.

References

[1] C.C. Griffioen, J.H. Evans, P.C. de Jong, A. van Veen. Nucl. Instrum. Meth. Phys. Res. B, **27** (3), 417 (1987). DOI: 10.1016/0168-583X (87)90522-2
[2] C.C. Griffioen, J.H. Evans, P.C. De Jong, A. Van Veen. Nucl. Instrum. Meth. Phys. Res., **28** (3), 360 (1987). DOI: 10.1016/0168-583X (87)90176-5
[3] V. Raineri, P.G. Fallica, G. Percolla, A. Battaglia, M. Barbagallo, S.U. Campisano. J. Appl. Phys., **78**, 3727 (1995). DOI: 10.1063/1.522860
[4] A. Ogura. Appl. Phys. Lett., **82** (25), 4480 (2003). DOI: 10.1063/1.1586783
[5] M. Hasanuzzaman, Y.M. Haddara, A.P. Knights. J. Appl. Phys., **112**, 064302 (2012). DOI: 10.1063/1.4751267
[6] K. Haynes, X. Hu, B.D. Wirth, C. Hatem, K.S. Jones. J. Appl. Phys., **124**, 165708 (2018). DOI: 10.1063/1.5053660
[7] J. H. Evans. Nucl. Instrum. Meth. Phys. Res. B, **196**, 125 (2002).
[8] P.A. Alexandrov, O.V. Emelyanova, S.G. Shemardov, D.N. Khmelenin, A.L. Vasiliev. Kristallografiya, **69** (3), 494 (2024) (in Russian). DOI: 10.31857/S0023476124030123
[9] R. Siegele, G.C. Weatherly, H.K. Haugen. Appl. Phys. Lett., **66** (11), 1319 (1995). DOI: 10.1063/1.113228
[10] P. Ericsson, S. Bengtsson. Appl. Phys. Lett., **71** (16), 2310 (1997). DOI: 10.1063/1.120058
[11] B.S. Li, C.H. Zhang, H.H. Zhang, Y. Li, G. Yin, J. Liu, Z. Liu, H.R. Liu, Z.X. Zhao, Y.Q. Han, Z.L. Yu, X.Q. Feng. Nucl. Instrum. Meth. B, **269**, 739 (2011). https://doi.org/10.1016/j.nimb.2010.11.079
[12] K. Ono, M. Mjamoto, H. Kurata, S. Takahashi, S. Maekawa. J. Appl. Phys., **126**, 135104 (2019). DOI: 10.1063/1.5118994
[13] X. Huang, Y. Xie, M. Balooch, S. Lubner, P. Hosemann. J. Appl. Phys., **132**, 025106 (2022). https://doi.org/10.1063/5.0096802

Translated by T.Zorina